Intraoperative Segmentation and Nonrigid Registration for Image Guided Therapy

Simon K. Warfield[1], Arya Nabavi[1,3], Torsten Butz[4], Kemal Tuncali[2], Stuart G. Silverman[2], Peter McL. Black[3], Ferenc A. Jolesz[1], and Ron Kikinis[1]

[1] Surgical Planning Laboratory
http://www.spl.harvard.edu
[2] Department of Radiology,
[3] Department of Surgery, Harvard Medical School and Brigham and Women's Hospital, 75 Francis St., Boston, MA 02115 USA,
[4] Signal Processing Laboratory, Swiss Federal Institute of Technology at Lausanne, 1015 Lausanne, Switzerland.
{warfield,arya,butz,ktuncali,jolesz,kikinis}@bwh.harvard.edu,
pmblack@bics.bwh.harvard.edu, sgsilverman@partners.org

Abstract. Our goal was to improve image guidance during minimally invasive image guided therapy by developing an intraoperative segmentation and nonrigid registration algorithm. The algorithm was designed to allow for improved navigation and quantitative monitoring of treatment progress in order to reduce the time required in the operating room and to improve outcomes.

The algorithm has been applied to intraoperative images from cryotherapy of the liver and from surgery of the brain. Empirically the algorithm has been found to be robust with respect to imaging characteristics such as noise and intensity inhomogeneity and robust with respect to parameter selection. Serial and parallel implementations of the algorithm are sufficiently fast to be practical in the operating room.

The contributions of this work are an algorithm for intraoperative segmentation and intraoperative registration, a method for quantitative monitoring of cryotherapy from real-time imaging, quantitative monitoring of brain tumor resection by comparison to a preoperative treatment plan and an extensive validation study assessing the reproducibility of the intraoperative segmentation. We have evaluated our algorithm with six neurosurgical cases and two liver cryotherapy cases with promising results. Further clinical validation with larger numbers of cases will be necessary to determine if our algorithm succeeds in improving intraoperative navigation and intraoperative therapy delivery and hence improves therapy outcomes.

1 Introduction

Image guided surgical techniques are used in operating rooms equipped with special purpose imaging equipment. The development of image guided surgical methods over the past decade has provided a major advance in minimally

S.L. Delp, A.M. DiGioia, and B. Jaramaz (Eds.): MICCAI 2000, LNCS 1935, pp. 176–185, 2000.

invasive therapy delivery. Early work such as that reviewed by Jolesz [1] has established the importance and value of image guidance through better determination of tumor margins, better localization of lesions, and optimization of the surgical approach.

Research in image guided therapy has been driven by the need for improved visualization. Qualitative judgements by experts in clinical domains have been relied upon as quantitative and automated assessment of intraoperative imaging data has not been possible in the past. In order to provide the surgeon or interventional radiologist with as rich a visualization environment as possible from which to derive such judgements, existing work has been concerned primarily with image acquisition, visualization and registration of intraoperative and preoperative data. Intraoperative segmentation has the potential to be a significant aid to the intraoperative interpretation of images and to enable prediction of surgical changes.

Earlier work has been a steady progression of improving image acquisition and intraoperative image processing. This has included increasingly sophisticated multimodality image fusion and registration. Clinical experience with image guided therapy in deep brain structures and with large resections has revealed the limitations of existing rigid registration and visualization approaches [1]. The deformations of anatomy that take place during such surgery are often better described as nonrigid and suitable approaches to capture such deformations are being actively developed by several groups (described below).

A number of imaging modalities have been used for image guidance. These include, amongst others, computed tomography (CT), ultrasound, digital subtraction angiography (DSA), and magnetic resonance imaging (MRI). Intraoperative MR imaging can acquire high contrast images of soft tissue anatomy which has proven to be very useful for image-guided therapy [2]. Multi-modality registration allows preoperative data that cannot be acquired intraoperatively, such as fMRI or nuclear medicine scans, to be visualized together with intraoperative data.

Gering et al. [3] described an integrated system allowing the ready visualization of intraoperative images with preoperative data, including surface rendering of previously prepared triangle models and arbitrary interactive resampling of 3D grayscale data. Multiple image acquisitions were presented in a combined visualization through rigid registration and trilinear interpolation. The system also allows for visualization of virtual surgical instruments in the coordinate system of the patient and patient image acquisitions. The system supports qualitative analysis based on expert inspection of image data and the surgeons expectation of what should be present (normal anatomy, patient's particular pathology, current progress of the surgery etc.)

Several groups have investigated intraoperative nonrigid registration, primarily for neurosurgical applications. The approaches can be categorized by those that use some form of biomechanical model (recent examples include [4, 5, 6]) and those that apply a phenomenological approach relying upon image related criteria (recent examples include [7, 8].)

We aimed to demonstrate that intraoperative segmentation is possible and adds significantly to the value of intraoperative imaging. Compared to registration of preoperative images and inspection of intraoperative images alone, intraoperative segmentation enables identification of structures not present in previous images (examples of such structures include the region of cryoablation or radiofrequency treatment area, surgical probes and changes due to resection), quantitative monitoring of the progress of therapy (including the ability to compare quantitatively with a preoperatively determined treatment plan) and intraoperative surface rendering for rapid 3D interactive visualization.

2 Method

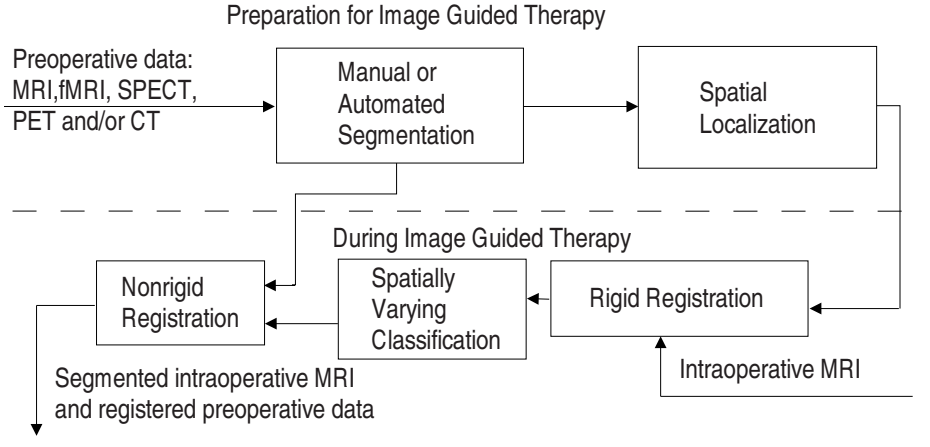

Fig. 1. Schema for Intraoperative Segmentation and Registration

In order to successfully segment intraoperative images, we have developed an image segmentation algorithm that takes advantage of an existing preoperative MR acquisition and segmentation to generate a patient-specific model for the segmentation of intraoperative data. The algorithm uses the segmentation of preoperative data as a template for the segmentation of intraoperative data. Figure 1 illustrates the processing steps that take place before and during the therapy procedure.

We have experimented for several years with a general image segmentation approach that uses a 3D digital anatomical atlas to provide automatic local context for classification [9, 10, 11]. The work described here extends our previous work to ensure its suitability for intraoperative segmentation. Rather than a generic digital anatomic atlas we propose here to use a segmented preoperative patient scan to derive a patient-specific anatomical model for intraoperative segmentation of new scans.

Since preoperative data is acquired before surgery, the time available for segmentation is longer. This means we can use segmentation approaches that are robust and accurate but are time consuming and hence impractical to use in the operating room. In our laboratory, preoperative data is segmented with a variety of manual [3], semi-automated [12] or automated [13, 11] approaches. We attempt to select the most robust and accurate approach available for a given clinical application. Each segmented tissue class is then converted into an explicit 3D volumetric spatially varying model of the location of that tissue class, by computing a saturated distance transform [14] of the tissue class. This model is used to provide robust automatic local context for the classification of intraoperative data in the following way.

During surgery, intraoperative data is acquired and the preoperative data (including any MRI/fMRI/PET/SPECT/MRA that is appropriate, the tissue class segmentation and the spatial localization model derived from it) is aligned with the intraoperative data using an MI based rigid registration method [15, 3]. The intraoperative image data then together with the spatial localization model forms a multichannel 3D data set. Each voxel is then a vector having components from the intraoperative MR scan, the spatially varying tissue location model and if relevant to the particular application, any of the other preoperative image data sets. For the first intraoperative scan to be segmented a statistical model for the probability distribution of tissue classes in the intensity and anatomical localization feature space is built. The statistical model is encoded implicitly by selecting groups of prototypical voxels which represent the tissue classes to be segmented intraoperatively (less than five minutes of user interaction). The spatial location of the prototype voxels is recorded and is used to update the statistical model automatically when further intraoperative images are acquired and registered. This multichannel data set is then segmented with a spatially varying classification [10, 13, 16].

Segmentation of intraoperative data helps to establish explicitly the regions of tissues that correspond in the preoperative and intraoperative data. It is then straightforward to apply our previously described [17, 18] and validated [19] multi-resolution elastic matching algorithm. Once the nonrigid transformation mapping from the preoperative to the intraoperative data has been established, the mapping is applied to each of the relevant preoperative data sets to bring them into alignment with the intraoperative scan.

3 Results

In this section illustrative segmentations and two validation experiments are presented. During interventional procedures in the liver and brain, intraoperative MRI (IMRI) data sets were acquired and stored. Our segmentation and nonrigid registration algorithm was applied to these data sets after therapy delivery in order to allow us to assess the robustness, accuracy and time requirements of the approach. In the future we intend to carry out segmentation, nonrigid regis-

tration and visualization using the approach described here during the interventional procedures with the goal of improving image guided therapy outcomes.

3.1 Intraoperative Segmentation for Neurosurgery

Figure 2 illustrates the segmentation of six neurosurgery cases using our intraoperative segmentation algorithm. In each case, several volumetric MRI scans were carried out during surgery. The first scan was acquired at the beginning of the procedure before any changes in the shape of the brain took place, and then over the course of surgery other scans were acquired as the surgeon checked the progress of tumor resection. The final scan in each sequence exhibits significant nonrigid deformation and loss of tissue due to tumor resection. In order to test our segmentation approach each subsequent scan was aligned to the first by maximization of mutual information and the first scan was manually segmented to act as an individualized anatomical model. The last scan in each sequence was then segmented with our new segmentation approach. The segmented brain and IMRI is shown in Figure 2. In order to check the quality of the segmentation, each segmentation was visually compared with the MRI from which it was derived. In each case the segmented brain closely matched the expected location.

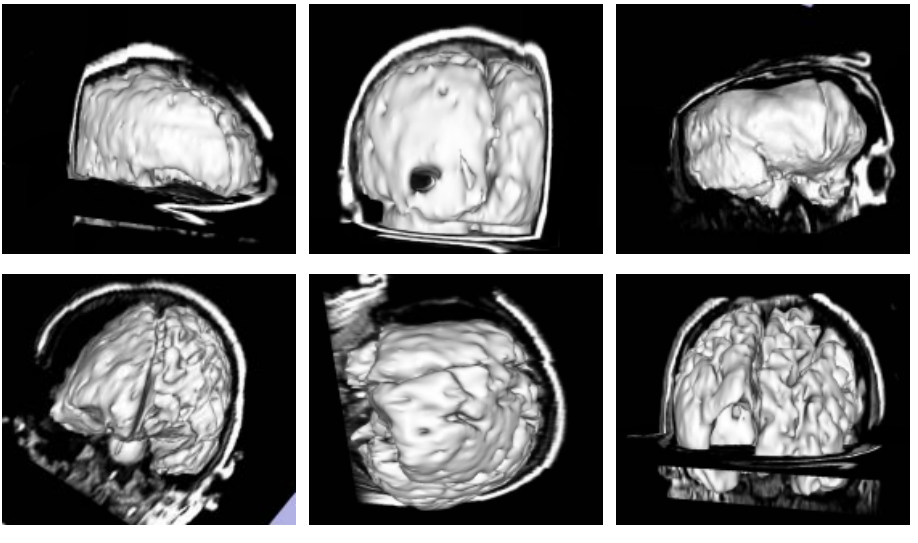

Fig. 2. Visualizations of intraoperative segmentation of brain tissue from six neurosurgery cases. Less than five minutes of user interaction was required for each segmentation. The segmented brain tissue is shown in white with surface rendering and the IMRI is texture mapped in planes along the coordinate axes. This allows ready comparison of the position of the segmented brain and the IMRI (skin appears bright, brain is gray closely matching the segmented brain border).

User Interaction and Computational Requirements Each brain segmentation of Figure 2 involves the segmentation of the entire 3D IMRI scan of 256x256x60 = 3,932,160 voxels (with voxel size 0.9375x0.9375x2.5mm^3.) Such a volume is acquired in approximately 10 minutes intraoperatively (a second scanning mode can acquire a 2D image in approximately 2 seconds). Less than five minutes of user interaction was required for each brain segmentation shown in Figure 2. On a Sun Microsystems Ultra-10 workstation with a 440MHz UltraSPARC-IIi CPU and 512MB RAM each brain tissue segmentation (excluding generation of spatial localization models which requires approximately 200 seconds and can be done preoperatively and excluding rigid registration which requires approximately 30 seconds using maximization of mutual information [15]) required less than 330 seconds to complete. As we have previously described, parallel tissue classification can achieve excellent speedups [20]. On a Sun Microsystems Ultra-80 server with 4 x 450MHz UltraSPARC-II CPUs and 2GB RAM, each brain tissue segmentation required less than 130 seconds to complete. This can be compared to a typical manual segmentation that can take 1800–3600 seconds and has significantly less reproducibility.

3.2 Intraoperative Segmentation for Liver Cryotherapy

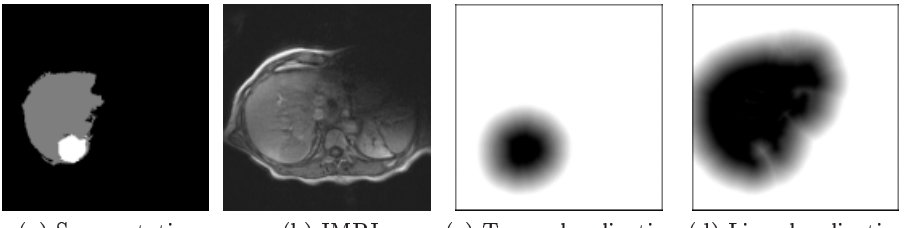

Fig. 3. IMRI of the liver and the segmentation of the liver and tumor. Three of the feature channels used to carry out the segmentation shown in (a) are shown in (b), (c) and (d).

Figure 3 shows IMRI of the liver and the segmentation of the liver and tumor. Intraoperative MRI has been used to guide percutaneous cryotherapy of liver tumors [21]. This figure illustrates the spatial localization of liver and tumor from a 3D volumetric preoperative segmentation (not shown) and indicates that isointense but different structures in the IMRI can be successfully segmented in the joint feature space formed with the IMRI intensity and spatial localization information.

3.3 Intraoperative Monitoring of Cryotherapy Iceball Formation

Figure 4 shows the intraoperative appearance of an iceball during cryotherapy of another case. Our intraoperative segmentation algorithm allowed rapid, robust

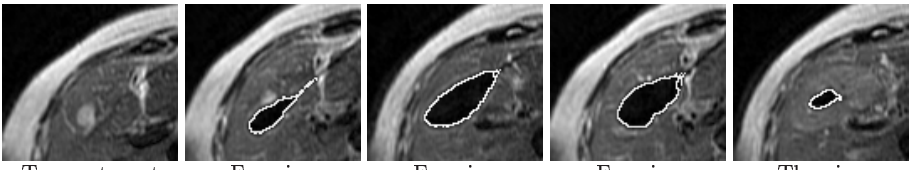

Fig. 4. Intraoperative imaging of iceball formation. The lesion is bright in the first image and the iceball grows to cover it. The iceball appears as a dark region in the liver, which grows while freezing and shrinks during thawing. The intraoperative iceball segmentation obtained with our method is indicated by the white outline.

and straightforward segmentation of the iceball. By comparing the segmentation of the iceball with a preoperative plan of the desired iceball size and location the therapy progress can be monitored quantitatively.

3.4 Validation Experiments

Key parameters in our segmentation algorithm are the prototype voxels which implicitly model the probability distribution of the intensities of tissues which are to be segmented and the alignment of the spatial localization models which form part of the feature space in which the tissue classification takes place. We studied the effect of variations in these key parameters upon the segmentation.

Reproducibility: Variations in Prototype Selection Table 1 records the variability of brain segmentation from a single neurosurgery case when the set of prototype voxels modeling the tissue characteristics is varied. The set of prototypes used for the segmentation was subsampled by randomly selecting 90% of the prototypes 100 times. Each of the 100 subsets simulates different user prototype selection. Each subset was used to segment the IMRI using the new method and the volume of the brain segmentation was recorded. The mean, minimum and maximum volume recorded are shown in the table along with the coefficient of variation (C.V.) of the volume of segmentation (which is less than 1%). This indicates the segmentation is extremely robust in the presence of variability in the prototype voxel selection.

Minimum volume	Maximum volume	Mean volume	C.V. (%)
401074 voxels	422440 voxels	414440 voxels	0.97

Table 1. Measures of variability of the volume of the brain (units are voxels) in repeated segmentations, with different selections of prototype voxels, from brain IMRI.

Reproducibility: Variations in Preoperative Model Alignment In order to determine the influence of the alignment of the preoperative segmentation upon the intraoperative segmentation, we selected a neurosurgery case and segmented the brain as described above. We then applied a set of translations and rotations to the preoperative segmentation so that it was no longer correctly registered to the IMRI to be segmented. For each translation and rotation we applied our segmentation method and obtained a segmentation of the brain. We then compared the volume of tissue segmented as brain for each misaligned position with that obtained with the correct alignment and recorded the ratio of the new segmentation volume to the original segmentation volume. The variation in segmentation with translations along each of the coordinate axes is shown in Figure 5. Similar results (not shown) were obtained for rotations around each of the coordinate axes.

Intrapatient registration with maximization of mutual information has a typical accuracy smaller than one voxel (in this case 0.9375x0.9375x2.5mm^3). The perturbation of the registration of the preoperative segmentation does not cause a significant change in the intraoperative segmentation until this misalignment reaches around ±10 mm, which indicates our intraoperative segmentation method is robust to misalignment errors and also to errors in the preoperative segmentation.

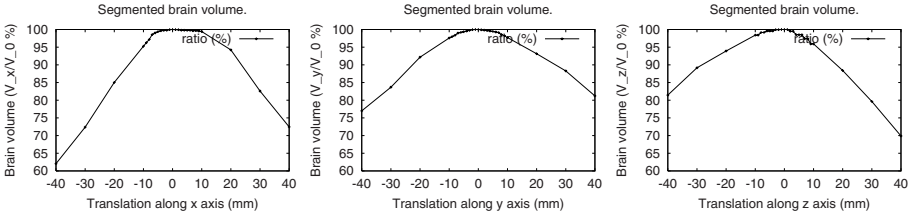

Fig. 5. Reproducibility of brain tissue segmentation as the spatial localization model is translated. The low variability in segmentation around the correct alignment indicates the segmentation is robust to misregistration and spatial localization errors.

4 Discussion and Conclusion

Our early experience with two liver cases and six neurosurgery cases indicates that our intraoperative segmentation algorithm is a robust and reliable method for intraoperative segmentation. It requires little user interaction, is robust to variation in the parameters that require interaction, and is sufficiently fast to be used intraoperatively.

The application of our previously described and validated nonrigid registration algorithm is enabled by intraoperative segmentation establishing the cor-

responding tissues in the data sets to be aligned. Further work is needed to characterize the accuracy and robustness of our nonrigid registration for intraoperative data, especially in the liver.

Intraoperative segmentation adds significantly to the value of intraoperative imaging. Compared to registration of preoperative images and inspection of intraoperative images alone, intraoperative segmentation enables identification of structures not present in previous images (examples of such structures include the region of cryoablation or RF treatment area, surgical probes and changes due to resection), quantitative monitoring of therapy application including the ability to compare quantitatively with a preoperatively determined treatment plan and intraoperative surface rendering for rapid 3D interactive visualization.

The contributions of this work are an algorithm for intraoperative segmentation and intraoperative registration, a method for quantitative monitoring of cryotherapy from real-time imaging, quantitative monitoring of brain tumor resection by comparison to a preoperative treatment plan and an extensive validation study assessing the reproducibility of the intraoperative segmentation. Empirically the algorithm has been found to be robust with respect to imaging characteristics such as noise and intensity inhomogeneity and robust with respect to parameter selection. Serial and parallel implementations of the algorithm are sufficiently fast to be practical in the operating room.

We have evaluated our algorithm with six neurosurgical cases and two liver cryotherapy cases. Further clinical validation with larger numbers of cases will be necessary to determine if our new approach succeeds in improving intraoperative navigation and intraoperative therapy delivery and hence improves therapy outcomes.

Acknowledgements: This investigation was supported by NIH P41 RR13218, NIH P01 CA67165 and NIH R01 RR11747.

References

[1] F. Jolesz, "Image-guided Procedures and the Operating Room of the Future," *Radiology*, vol. 204, pp. 601–612, May 1997.

[2] P. M. Black, T. Moriarty, E. Alexander, P. Stieg, E. J. Woodard, P. L. Gleason, C. H. Martin, R. Kikinis, R. B. Schwartz, and F. A. Jolesz, "The Development and Implementation of Intraoperative MRI and its Neurosurgical Applications," *Neurosurgery*, vol. 41, pp. 831–842, April 1997.

[3] D. Gering, A. Nabavi, R. Kikinis, W. Grimson, N. Hata, P. Everett, F. Jolesz, and W. Wells, "An Integrated Visualization System for Surgical Planning and Guidance using Image Fusion and Interventional Imaging," in *MICCAI 99: Proceedings of the Second International Conference on Medical Image Computing and Computer Assisted Intervention*, pp. 809–819, Springer Verlag, 1999.

[4] A. Hagemann, K. Rohr, H. Stiel, U. Spetzger, and J. Gilsbach, "Biomechanical modeling of the human head for physically based, non-rigid image registration," *IEEE Transactions On Medical Imaging*, vol. 18, no. 10, pp. 875–884, 1999.

[5] O. Skrinjar and J. Duncan, "Real time 3D brain shift compensation," in *IPMI'99*, pp. 641–649, 1999.

[6] M. Miga, K. Paulsen, J. Lemery, A. Hartov, and D. Roberts, "In vivo quantification of a homogeneous brain deformation model for updating preoperative images during surgery," *IEEE Transactions On Medical Imaging*, vol. 47, pp. 266–273, February 1999.

[7] D. Hill, C. Maurer, R. Maciunas, J. Barwise, J. Fitzpatrick, and M. Wang, "Measurement of intraoperative brain surface deformation under a craniotomy," *Neurosurgery*, vol. 43, pp. 514–526, 1998.

[8] N. Hata, *Rigid and deformable medical image registration for image-guided surgery*. PhD thesis, University of Tokyo, 1998.

[9] S. Warfield, J. Dengler, J. Zaers, C. R. Guttmann, W. M. Wells III, G. J. Ettinger, J. Hiller, and R. Kikinis, "Automatic identification of Grey Matter Structures from MRI to Improve the Segmentation of White Matter Lesions," *Journal of Image Guided Surgery*, vol. 1, no. 6, pp. 326–338, 1995.

[10] S. K. Warfield, M. Kaus, F. A. Jolesz, and R. Kikinis, "Adaptive Template Moderated Spatially Varying Statistical Classification," in *MICCAI 98: First International Conference on Medical Image Computing and Computer-Assisted Intervention*, pp. 231–238, Springer-Verlag, Heidelberg, Germany, October 11–13 1998.

[11] M. R. Kaus, S. K. Warfield, A. Nabavi, E. Chatzidakis, P. M. Black, F. A. Jolesz, and R. Kikinis, "Segmentation of MRI of meningiomas and low grade gliomas," in *MICCAI 99: Second International Conference on Medical Image Computing and Computer-Assisted Intervention* (C. Taylor and A. Colchester, eds.), pp. 1–10, Springer-Verlag, Heidelberg, Germany, 1999.

[12] R. Kikinis, M. E. Shenton, G. Gerig, J. Martin, M. Anderson, D. Metcalf, C. R. G. Guttmann, R. W. McCarley, W. E. Lorenson, H. Cline, and F. Jolesz, "Routine Quantitative Analysis of Brain and Cerebrospinal Fluid Spaces with MR Imaging," *Journal of Magnetic Resonance Imaging*, vol. 2, pp. 619–629, 1992.

[13] S. K. Warfield, M. Kaus, F. A. Jolesz, and R. Kikinis, "Adaptive, Template Moderated, Spatially Varying Statistical Classification," *Medical Image Analysis*, vol. 4, no. 1, pp. 43–55, 2000.

[14] I. Ragnemalm, "The Euclidean distance transform in arbitrary dimensions," *Pattern Recognition Letters*, vol. 14, pp. 883–888, 1993.

[15] W. M. Wells, P. Viola, H. Atsumi, S. Nakajima, and R. Kikinis, "Multi-modal volume registration by maximization of mutual information," *Medical Image Analysis*, vol. 1, pp. 35–51, March 1996.

[16] R. O. Duda and P. E. Hart, *Pattern Classification and Scene Analysis*. John Wiley & Sons, Inc., 1973.

[17] J. Dengler and M. Schmidt, "The Dynamic Pyramid – A Model for Motion Analysis with Controlled Continuity," *International Journal of Pattern Recognition and Artificial Intelligence*, vol. 2, no. 2, pp. 275–286, 1988.

[18] S. K. Warfield, A. Robatino, J. Dengler, F. A. Jolesz, and R. Kikinis, "Nonlinear Registration and Template Driven Segmentation," in *Brain Warping* (A. W. Toga, ed.), ch. 4, pp. 67–84, Academic Press, San Diego, USA, 1999.

[19] D. V. Iosifescu, M. E. Shenton, S. K. Warfield, R. Kikinis, J. Dengler, F. A. Jolesz, and R. W. McCarley, "An Automated Registration Algorithm for Measuring MRI Subcortical Brain Structures," *NeuroImage*, vol. 6, pp. 12–25, 1997.

[20] S. K. Warfield, F. A. Jolesz, and R. Kikinis, "Real-Time Image Segmentation for Image-Guided Surgery," in *Supercomputing 1998*, pp. 1114:1–14, November 1998.

[21] S. G. Silverman, K. Tuncali, D. F. Adams, E. vanSonnenberg, K. H. Zou, D. F. Kacher, P. R. Morrison, and F. A. Jolesz, "MRI-Guided percutaneous cryotherapy of liver tumors: initial experience," *Radiology*. In press.